Terminal Titanyl Complexes of Tri- and Tetrametaphosphate: Synthesis, Structures, and Reactivity with Hydrogen Peroxide

Citation: Stauber, Julia M., and Christopher C. Cummins. "Terminal Titanyl Complexes of Tri- and Tetrametaphosphate: Synthesis, Structures, and Reactivity with Hydrogen Peroxide." Inorganic Chemistry, vol. 56, no. 5, Mar. 2017, pp. 3022–29. © 2017 American Chemical Society

As Published: http://dx.doi.org/10.1021/acs.inorgchem.6b03149

Publisher: American Chemical Society

Persistent URL: http://hdl.handle.net/1721.1/114511

Version: Author's final manuscript: final author's manuscript post peer review, without publisher's formatting or copy editing

Terminal Titanyl Complexes of Tri- and Tetrametaphosphate: Synthesis, Structures, and Reactivity with Hydrogen Peroxide

Julia M. Stauber, and Christopher C. Cummins*

Department of Chemistry, Massachusetts Institute of Technology, 77 Massachusetts Avenue, Cambridge, Massachusetts 02139

Received February 1, 2017; E-mail: ccummins@mit.edu

ABSTRACT: The synthesis and characterization of tri- and tetrametaphosphate titanium(IV) oxo and peroxo complexes is described. Addition of 0.5 equiv $[OTi(acac)_2]_2$ to dihydrogen tetrametaphosphate ($[P_4O_{12}H_2]^{2-}$) and monohydrogen trimetaphosphate ($[P_3O_9H]^{2-}$) provided a bis(μ_2,κ^2,κ^2) tetrametaphosphate titanyl dimer, $[OTiP_4O_{12}]_2^{4-}$ (**1**, 70% yield), and a trimetaphosphate titanyl acetylacetonate complex, $[OTiP_3O_9(acac)]^{2-}$ (**2**, 59% yield). Both **1** and **2** have been structurally characterized, crystallizing in the triclinic $P\bar{1}$ and monoclinic $P2_1$ space groups, respectively. These complexes contain Ti≡O units with distances of 1.624(7) and 1.644(2) Å, respectively, and represent rare examples of structurally characterized terminal titanyls within an all-oxygen coordination environment. Complexes **1** and **2** react with hydrogen peroxide to produce the corresponding peroxotitanium(IV) metaphosphate complexes, $[O_2TiP_4O_{12}]_2^{4-}$(**3**, 61% yield), and $[O_2TiP_3O_9(acac)]^{2-}$ (**4**, 65% yield), respectively. Both **3** and **4** have been characterized by single crystal X-ray diffraction studies, and their solid-state structures are presented. Complex **3** functions as an oxygen atom transfer (OAT) reagent capable of oxidizing phosphorus(III) compounds ($P(OMe)_3$, PPh_3) and SMe_2 at ambient temperature to result in the corresponding organic oxide with regeneration of dimer **1**.

■ INTRODUCTION

Oxidative degradation of organic ligands is a challenge faced in many synthetic systems as most oxidation catalysts require ligand environments capable of supporting reactive high-valent metal oxos.[1] Furthermore, the deactivation of high-valent metal oxos through the formation of unreactive dimeric or oligomeric μ-oxo species is an additional common challenge.[2] In heterogeneous systems, these issues are circumvented through site isolation of discrete metal oxos within inorganic matrices that function as thermodynamically stable ligand environments.[3,4] An example of one such system is Enichem's highly efficient TS-1 oxidation catalyst,[5,6] a titanium based microporous molecular sieve in which Ti(IV) ions are isolated within an entirely silicate based framework.[7]

The success of TS-1 and other industrial oxidation catalysts has driven synthetic chemists to study molecular models of heterogeneous systems. Kortz et al. have studied titanium(IV) oxo[8] and hydroxo[9] substituted polyoxometalates (POMs) as models of Ti single site catalysts due to the structural analogy of POMs and metal oxide surfaces. These oxidatively stable titanium(IV) POM complexes have served as molecular models for studying mechanisms of selective oxidation.[10] With the present work, we sought to investigate the suitability of similarly all-inorganic metaphosphate rings (cyclic oligomers of the PO_3^- anion) for stabilization of the titanyl functional group in an all-oxygen coordination environment.

■ RESULTS AND DISCUSSION

Synthesis of Titanyl Complexes. The $[PPN]^+$ salts of both dihydrogen tetrametaphosphate ($[PPN]_2[P_4O_{12}H_2]$) and monohydrogen trimetaphosphate ($[PPN]_2[P_3O_9H]$) can be prepared in multigram quantities under open air conditions by protonation of their corresponding metaphosphate salts with strong acid.[11,12] We have previously shown that the $[P_4O_{12}H_2]^{2-}$ acid can be used to synthesize metal complexes through protonolysis of basic ligands such as $[N(SiMe_3)_2]^-$, leading to the facile preparation of tetrametaphosphate tin(II) ($[SnP_4O_{12}]^{2-}$) and chromium(II) ($[CrP_4O_{12}]_2^{4-}$) salts.[11] Employing the strategy of protolytic ligand replacement, we chose to investigate the reactivity of both the $[P_4O_{12}H_2]^{2-}$ and $[P_3O_9H]^{2-}$ acids with titanyl bis(acetylacetonate) ($[OTi(acac)_2]_2$).[13] Even though its structure is dimeric, $[OTi(acac)_2]_2$ provides a commercially available source of the titanyl (OTi) unit that bears basic ligands potentially susceptible to protolytic replacement by the metaphosphate acids. Acetylacetone, the byproduct formed through protonation, is easily separable from the desired metaphosphate salts, making the preparation of titanyl metaphosphate complexes convenient and straightforward.

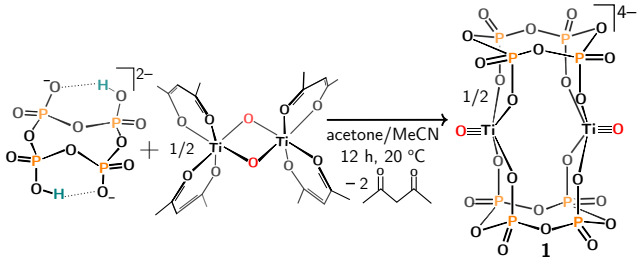

Scheme 1. Synthetic protocol for the preparation of $[PPN]_4[OTiP_4O_{12}]_2$ ($[PPN]_4$[**1**]).

Treatment of 1 equiv $[PPN]_2[P_4O_{12}H_2]$ with 0.5 equiv $[OTi(acac)_2]_2$ in an acetone/MeCN mixture at 23 °C afforded a new species, $[OTiP_4O_{12}]_2^{4-}$ (**1**), after 12 h of reaction time (Scheme 1). Analytically pure X-ray quality crystals of $[PPN]_4$[**1**] were easily isolated from the acetylacetone byproduct in 70% yield after concentration of the crude reaction mixture and storage at 23 °C overnight. The identity of **1** was established through an X-ray diffraction study, and the solid-state structure is shown in Figure S58 (left). The $^{31}P\{^1H\}$ NMR spectrum of dimer **1** features a singlet located at δ –27.55 ppm (Figure S1), which is shifted slightly upfield from that of $[P_4O_{12}H_2]^{2-}$. The Ti≡O stretching frequency observed by FTIR at 969 cm^{-1} (Figure S5) is in line with data reported for other terminal titanyl complexes reported in the literature,[14–17] and falls within the characteristic range (972–890 cm^{-1}) associated with the Ti≡O oscillator.[18] The formula of the $[OTiP_4O_{12}]_2^{4-}$ anion was also confirmed by ESI-MS(–) with a m/z value of 189.88 (Figure S7, calc'd: 189.89).

$[PPN]_4$[**1**] crystallized in the triclinic space group, $P\bar{1}$, with two $[PPN]^+$ cations and half of the $[OTiP_4O_{12}]_2^{4-}$ dimer in the asym-

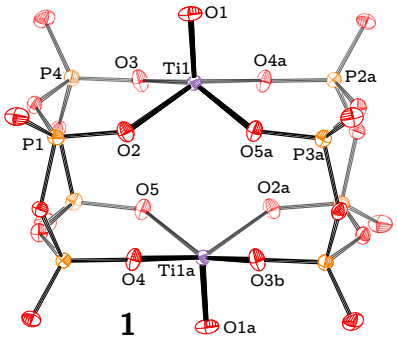

Figure 1. Solid-state structure of $[OTiP_4O_{12}]_2^{4-}$ (**1**) $[OTiP_3O_9(acac)]^{2-}$ rendered with PLATON[25] with thermal ellipsoids at the 50% probability level, and with $[PPN]^+$ cations and solvent molecules of crystallization omitted for clarity. Selected interatomic distances (Å) and angles (°): Ti1-O1 1.6252(13), Ti1-O2 1.9909(12), Ti1-O3 1.9939(13), Ti1-O4a 1.9844(13), Ti1-O5a 2.0014(13), Ti1-Ti1a 4.233(9), Σ(O_{eq}-Ti-O_{eq}) 341.8(9).

metric unit. As shown in Figure 1, the complex adopts a $[MP_4O_{12}]_2$ coordination geometry in which two tetrametaphosphate rings form a cofacial sandwich around the pair of titanyl ions resembling the structure of $[Cp^*TiP_4O_{12}]_2^{2-}$ reported by Ishii et al.[19] We reported previously that the chromium(II) complex of tetrametaphosphate forms just such a dimeric cofacial sandwich.[11] In **1**, the titanium centers reside 0.559 Å above the equatorial four membered oxygen plane of the tetrametaphosphate such that two κ^2 $[P_4O_{12}]^{4-}$ ligands bridge each Ti center to approximate D_{2h} point group symmetry. Dimer **1** contains a Ti···Ti distance of 4.233(9) Å, with a titanyl Ti≡O distance of 1.624(7) Å. While structurally characterized anionic titanium(IV) oxo complexes are rare,[20,21] the observed Ti≡O distance in **1** agrees well with corresponding metrical parameters reported for other neutral titanium(IV) oxo complexes with distances spanning 1.61 to 1.68 Å.[22] The Ti≡O distance observed in **1** is consistent with triple bond character as predicted by the titanium and oxygen triple bond covalent radii,[23] as well as the electronic considerations associated with d^0 transition metal oxos within tetragonal ligand fields.[24]

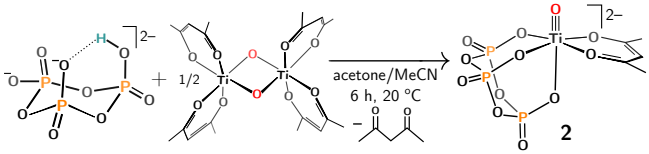

Scheme 2. Synthetic protocol for the preparation of $[PPN]_2[OTiP_3O_9(acac)]$ ($[PPN]_2$[**2**]).

As in the case of dihydrogen tetrametaphosphate, the $[PPN]_2[P_3O_9H]$ acid reacted with 0.5 equiv $[OTi(acac)_2]_2$ in an acetone/MeCN mixture under open air conditions to generate a titanyl metaphosphate complex, $[PPN]_2[OTiP_3O_9(acac)]$ ($[PPN]_2$[**2**], Scheme 2, Figure 2), with loss of one equiv acetylacetone. Complex **2** was isolated in 59% yield by crystallization through concentration of the crude reaction mixture and allowing the resulting solution to stand at 23 °C. After 12 h, large colorless crystals formed that were isolated and washed with acetone to afford analytically pure $[PPN]_2$[**2**].

The $^{31}P\{^1H\}$ NMR spectrum of **2**, recorded in acetonitrile, features a singlet located at δ –18.43 ppm that is assigned to the three phosphorus atoms of the $[P_3O_9]^{3-}$ ligand (Figure S8). The presence of a single broad signal can be ascribed to rapid rotation of the $[P_3O_9]^{3-}$ unit on the NMR time scale in solution, and is therefore represented as a weighted average. Collection of the $^{31}P\{^1H\}$ NMR spectrum at –35 °C resolved the broad singlet into a doublet and a triplet with an AX_2 splitting pattern located at δ –19.13 ($^2J_{PP}$ = 17.2 Hz) and –18.20 ppm ($^2J_{PP}$ = 17.2 Hz) in a 2:1 integral ratio (Figure S29). The doublet corresponds to the phosphorus atoms flanking the two equatorially bound oxygen atoms, and the triplet is assigned to the phosphorus bound to the axially coordinated oxygen atom of the $[P_3O_9]^{3-}$ ligand.

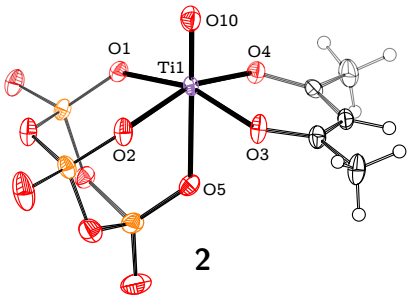

Figure 2. Solid-state structure of $[OTiP_3O_9(acac)]^{2-}$ (**2**) rendered with PLATON[25] with thermal ellipsoids at the 50% probability level, and with $[PPN]^+$ cations and solvent molecules of crystallization omitted for clarity. Selected interatomic distances (Å) and angles (°): Ti1-O10 1.644(2), Ti1-O1 2.033(2), Ti1-O2 2.0491(18), Ti1-O3 2.0145(19), Ti1-O4 2.0113(19), Ti1-O5 2.3211(19), Σ(O_{eq}-Ti-O_{eq}) 355.08(2).

An X-ray diffraction study confirmed the solid-state structure of **2** as a terminal titanyl complex with one $[P_3O_9]^{3-}$ and one acetylacetonate ligand bound to the titanium(IV) center to complete its entirely oxygen based octahedral coordination environment. Figure 2 displays a thermal ellipsoid plot of the anion from the $[PPN]_2$[**2**] salt. As a result of the strong trans influence imparted by the oxo ligand,[26] the Ti1–O5 distance of 2.3211(19) Å is significantly longer than expected for a Ti–O single bond (1.99 Å) as predicted by the titanium and oxygen single bond covalent radii,[23] suggesting this interaction is at best a weak one and that O5 may be simply in proximity of the Ti center by virtue of being part of the trimetaphosphate ring. Consistent with multiple bonding to a terminal oxo ligand, the IR spectrum of **2** displays the Ti≡O oscillator at ν = 953 cm^{-1} (Figure S11). This stretching frequency is 16 cm^{-1} lower in energy than that of **1**, and consistent with the slightly longer Ti≡O distance of **2** (1.644(2) Å) compared with that of **1** (1.6252(13) Å). In contrast to **2**, the position trans to the oxo ligand is vacant in dimer **1**, and thus **1** should be able to maximize the Ti≡O multiple bonding in accord with both its shorter bond distance and higher energy stretching frequency. The formula of **2** was also confirmed by ESI-MS(–) with a m/z value of 300.91 (Figure S14, calc'd: 300.82), which corresponds to the monoanionic complex, $[OTiP_3O_9]^-$, with loss of the $acac^-$ ligand under ESI-MS(–) conditions.

Dimer **1** was prepared under open atmosphere conditions and is air stable both in solution and as a solid. Dimer **1**, however, reacted with excess water (ca. 50–100 eq) in acetonitrile at 23 °C over the course of 5 min to form a new species exhibiting a higher order splitting pattern in its $^{31}P\{^1H\}$ NMR spectrum consistent with an

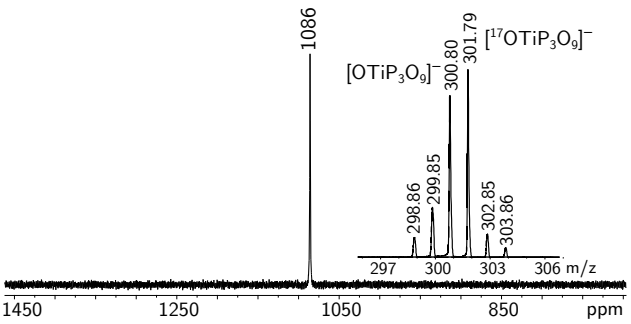

Figure 3. ^{17}O NMR spectrum of **2** after treatment with excess (40 eq) $^{17}OH_2$ (MeCN, 68 MHz, 20 °C, externally referenced to D_2O). Inset: ESI-MS(–) of **2** after treatment with excess $^{17}OH_2$ (MeCN, 3200 V).

$A_2A'_2B_2B'_2$ system (Figure S38).[27] Although the identity of this new species has not yet been confirmed, we propose that this product is a bimetallic titanium(IV) complex in which one of the Ti≡O units has reacted with H_2O to form two hydroxo ligands, while the other titanyl unit of dimer **1** is preserved (O≡Ti/Ti(OH)$_2$). When an acetonitrile solution containing this species was heated to 80 °C under vacuum, the $^{31}P\{^1H\}$ NMR spectrum of the resulting residue shows resonances corresponding to dimer **1**, revealing the reversibility of the aquation reaction (Figure S43). When a solution of **1** with excess water was allowed to stand at 23 °C for 12 h, complete conversion of the initial species to a new product was observed (Figure S40).

To gain more insight into the identity of these products, a reaction was carried out using ^{17}O enriched water. The ^{17}O NMR spectrum of an acetonitrile solution of **1** treated with excess (ca. 40 eq) $^{17}OH_2$ displays signals located at δ 1060 and 930 ppm (Figure S41), which fall within the range expected for terminal titanium(IV) oxo (1000–1100 ppm)[15,28,29] and hydroxo ligands (700-1000 ppm),[29] respectively, and are in line with our assignment of this species as the mixed O≡Ti/Ti(OH)$_2$ bistetrametaphosphate complex. When a sample was permitted to age for 12 h, these resonances were observed to decrease in intensity with new signals appearing at δ 758 and 566 ppm (Figure S42). These new signals are found within the region expected for Ti(IV) μ^2–O (650–850 ppm) and μ^3-O bridged species (450–600 ppm),[30] suggesting that after an extended period of time in the presence of a large excess of H_2O, dimer **1** is converted to μ-oxo bridged oligomers.

Complex **2** exhibits similar behavior to dimer **1** in being air stable in both the solid state, and in solution. In contrast to **1**, however, **2** is stable to excess water as judged by the unchanged ^{31}P NMR spectrum when a sample was left to stand in the presence of water (ca. 200 equiv) over the course of 24 h in acetonitrile (Figure S30). The water stability of **2** afforded the opportunity to study the titanyl oxygen exchange with $^{17}OH_2$ and $^{18}OH_2$ by ESI-MS(–) and ^{17}O NMR spectroscopy. Comba and Merbach have reported that the oxygen exchange rate for terminal oxo ligands in systems of hydrolyzed Ti(IV) is extremely fast as measured by ^{17}O NMR fast-injection and line-broadening techniques.[29] Consistent with these studies, the titanyl oxygen of complex **2** exchanged readily with both $^{18}OH_2$ and $^{17}OH_2$ as evaluated by ESI-MS(–) studies. As a result of this facile exchange, a ^{17}O NMR spectrum of **2** (Figure 3) was obtained after spiking a saturated acetonitrile solution of the compound with $^{17}OH_2$ (ca. 40 eq). The solution ^{17}O NMR spectrum displays one sharp signal located at δ 1086 ppm that is assigned as the -yl oxygen of **2**, and consistent with ^{17}O NMR studies of related terminal titanyl complexes.[15,28]

The formation of **1** and **2** from [OTi(acac)$_2$]$_2$ is noteworthy in illustrating that the tri- and tetrametaphosphates are capable of breaking up the titanium(IV) bis-μ-oxo core of [OTi(acac)$_2$]$_2$ to result in the formation of terminal Ti≡O units. Titanium(IV) oxo species are typically susceptible to hydrolysis in the presence of moist air as they have the propensity to dimerize and oligomerize forming unreactive species containing Ti–O–Ti linkages,[3,29] so the formation of a well-defined, air-stable terminal titanyl complex is unusual. Structurally characterized examples of complexes containing terminal titanyl units are known and typically contain nitrogen based macrocyclic ligands[31,32] such as porphyrins,[16] phthalocyanines,[33] and tacn derivatives (tacn = 1,4,7-triazacyclononane);[17,34] however, examples containing an oxygen-only coordination environment at titanium are extremely rare.[35] Such examples include $[OTi(OSMe_2)_5]^{2+}$,[36] and $[OTi(CO_3)_3]^{4-}$[37] complexes, and a sandwich-type 8-tungsto-2-arsenate(III) POM system ($[(OTi)_2(\alpha\text{-}AsW_9O_{33})_2]^{4-}$).[8] Additionally, direct evidence for the formation of terminal $[O{\equiv}Ti(aq)]^{2+}$ units in dilute acidic aqueous solutions of Ti(IV) has been observed.[29] The IR spectrum of such a solution contains a band at 975 cm^{-1} attributed to the Ti≡O vibration, while the ^{17}O NMR spectrum features a resonance located at δ 1028 ppm that is assigned to the -yl oxygen. These data are in line with the IR and ^{17}O NMR spectroscopic signatures of complexes **1** and **2**, suggesting that the ligand field exerted by metaphosphates may be similar to that of water.

Reactivity of Titanyl Complexes with Hydrogen Peroxide. The conversion of titanium(IV) oxo to titanium(IV) η^2-peroxo complexes through reaction with H_2O_2 is a well understood transformation[38] that has been thoroughly studied in both molecular[39,40] and heterogeneous[41] systems. This reactivity is of particular interest as hydrogen peroxide is used with many titanium silicate systems in catalytic oxidation reactions of organic substrates.[6,41–43] This transformation is not only relevant to oxidation processes, but because these reactions are typically accompanied by the appearence of an intense orange color, titanyl reactivity with hydrogen peroxide has been the basis for a colorimetric H_2O_2 sensing technology.[44]

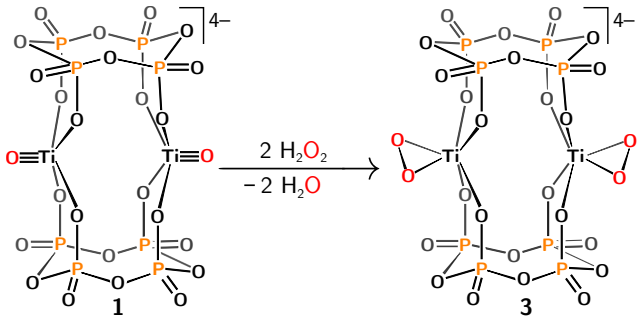

Scheme 3. Treatment of $[OTiP_4O_{12}]_2^{4-}$ (**1**) with 2 equiv H_2O_2 to yield $[O_2TiP_4O_{12}]_2^{4-}$ (**3**) with loss of 2 equiv H_2O.

Treatment of dimer **1** with 2 equiv urea·H_2O_2 (UHP) or $Me_3SiOOSiMe_3$ in acetonitrile resulted in a color change from colorless to orange, concomitant with the clean formation of the corresponding tetrametaphosphate peroxotitanium(IV) dimer ($[O_2TiP_4O_{12}]_2^{4-}$, **3**) with loss of 2 equiv H_2O or $Me_3SiOSiMe_3$, respectively. When UHP was used as the peroxide source (Scheme 3), the reaction was complete within 10 min, while the corresponding reaction with $Me_3SiOOSiMe_3$ was much more sluggish and required 12 h for completion. Both reactions were monitored with ^{31}P NMR spectroscopy wherein progress was associated with growth in of a singlet at δ –28.13 ppm (Figure S15). Additionally, the reaction was followed by UV-Vis spectroscopy by noting the appearance and growth of the absorption located at λ_{max} = 379 nm (Figure S20). The product was isolated (61% yield) as orange blocks obtained by layering diethyl ether onto an acetonitrile solution of the complex.

An X-ray diffraction study confirmed the identity of this product as a peroxotitanium(IV) κ^2 tetrametaphosphate dimer $[PPN]_4[O_2TiP_4O_{12}]_2$ (**3**), with the peroxo ligands bound η^2 to each titanium center. Figure 4 (left) shows a thermal ellipsoid plot of the anion from this salt. The O10-O20 peroxo ligand is disordered over two positions in which the major part lies in the O2–Ti1–O4a plane. A crystallographic mirror plane relates the two halves of the molecule such that the major part of the symmetry-generated O10b-O20b peroxo ligand lies in the O4-Ti1b-O2a plane. The complex contains Ti–O_{peroxo} and O–O distances of 1.795(8), 1.815(8) and 1.486(6) Å, respectively. These distances are in accord with data for related peroxotitanium(V) complexes reported in the literature.[21,40] The identity of **3** was also confirmed by ESI-MS(–), with a m/z value of 197.95 (Figure S21, calc'd, 197.89). The Ti≡O

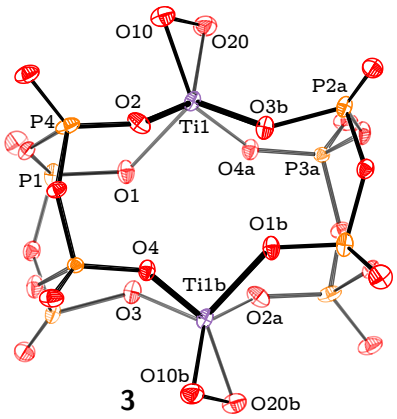

Figure 4. Solid-state structure of $[O_2TiP_4O_{12}]_2^{4-}$ (**3**) rendered with PLATON[25] with thermal ellipsoids at the 50% probability level, and with $[PPN]^+$ cations and solvent molecules of crystallization omitted for clarity. Selected interatomic distances (Å) and angles (°): Ti1-O10 1.815(8), Ti1-O20 1.795(8), Ti1-O1 1.896(13), Ti1-O2 1.935(12), Ti1-O3b 1.986(13), Ti1-O4a 1.963(12), O20-O10 1.486(6), Ti1-Ti1b 4.23(1), Σ(O_{eq}-Ti-O_{eq}) 352.0(7).

vibration at 969 cm^{-1} in the IR spectrum of **1** is absent in the spectrum of **3**, and a new stretch attributed to the peroxo O–O vibration is located at 856 cm^{-1} (Figure S18), and is consistent with a side-on η^2 coordination mode.[45] The strong absorption at λ_{max} = 379 nm in the UV-Vis spectrum of **3** is assigned to the $p\pi(O_2)\rightarrow d\pi(Ti)$ ligand to metal charge-transfer (LMCT) transition,[46] and compares well with other LMCT bands that have been observed for similar peroxotitanium(IV) complexes.[45–47] Like **1**, dimer **3** is air stable in both the solid state and in solution.

When the reaction of **1** with UHP was monitored by ^{31}P NMR spectroscopy at 5 °C in acetonitrile, an intermediate evincing an $A_2A_2'B_2B_2'$ splitting pattern (Figure S35) was observed before complete conversion to **3** occurred. This intermediate is assigned as the O≡Ti/Ti(O–O) bistetrametaphosphate complex, and completely converts to complex **3** after 80 min at 5 °C, and can only be observed at low temperature (≤ 5 °C).

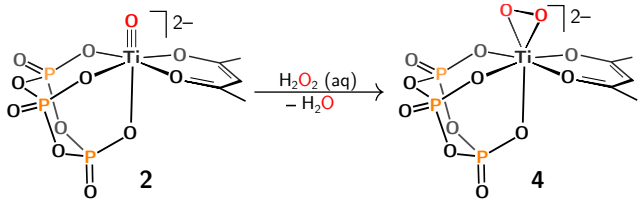

Scheme 4. Reaction of $[OTiP_3O_9(acac)]^{2-}$ (**2**) with H_2O_2 to yield $[O_2TiP_3O_9(acac)]^{2-}$ (**4**) with loss of H_2O.

Complex **2** also reacted cleanly with H_2O_2(aq) or $Me_3SiOOSiMe_3$ to generate a peroxotitanium(IV) trimetaphosphate acetylacetonate complex, $[PPN]_2[O_2TiP_3O_9(acac)]$ ($[PPN]_2$[**4**], Scheme 4, Figure 5), which was isolated in 65% yield after crystallization. **4** is characterized by a sharp singlet in its $^{31}P\{^1H\}$ NMR spectrum located at δ –17.73 ppm (Figure S22), a strong stretch at ν_{O-O} = 903 cm^{-1} in its IR spectrum (Figure S25), and an absorption located at λ_{max} = 403 nm (Figure S27, ε = 674 $M^{-1}cm^{-1}$) in the visible region of the electromagnetic spectrum. Crystals of $[PPN]_2$[**4**] suitable for an X-ray diffraction study were grown as orange blocks obtained by layering Et_2O onto an acetonitrile solution of the complex. $[PPN]_2$[**4**] crystallized in the monoclinic space group $P2_1$, and Figure 5 shows a thermal ellipsoid plot of the anion that displays the peroxo ligand oriented in an η^2 binding mode in which the O-O moiety is coincident with the O2–Ti1–O3 plane of the $[P_3O_9]^{3-}$ and $acac^-$ ligands. The structure determination revealed unremarkable Ti–O_{peroxo} and O–O

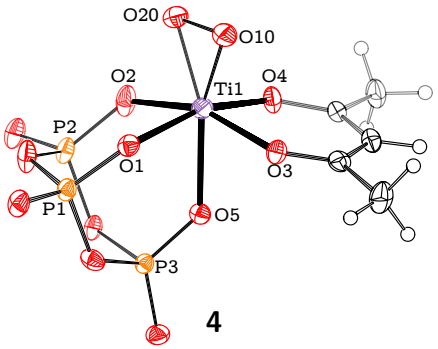

Figure 5. Solid-state structure of $[O_2TiP_3O_9(acac)]^{2-}$ (**4**) rendered with PLATON[25] with thermal ellipsoids at the 50% probability level, and with $[PPN]^+$ cations and solvent molecules of crystallization omitted for clarity. Selected interatomic distances (Å) and angles (°): Ti1-O20 1.850(4), Ti1-O10 1.823(5), Ti1-O1 2.063(3), Ti1-O2 2.048(2), Ti1-O3 2.040(2), Ti1-O4 1.997(2), Ti1-O5 2.166(2), O10-O20 1.443(6), Σ(O_{eq}-Ti-O_{eq}) 353.9(8).

distances of 1.850(4), 1.823(5), and 1.443(6) Å, respectively.

Examples of molecular peroxotitanium(IV) complexes that serve as oxidants towards organic substrates[46] are rare due to the well documented stability of the titanium-peroxo structural unit, and therefore its corresponding lack of oxidizing capacity.[6,48] It is instead believed that titanium(IV) hydroperoxo species play the active role in substrate oxidation within heterogeneous systems,[10,43,49] and therefore the preparation of well-defined titanium hydroperoxo complexes has been targeted by synthetic chemists.[50]

We were unable to observe a stable titanium(IV) hydroperoxo complex, and **1** and **2** did not show any signs of catalytic activity toward organic substrates in the presence of H_2O_2 (See Section 13 in the Supporting Information for experimental details). Both results are likely due to the rapid conversion of **1** and **2** to **3** and **4**, respectively, upon addition of H_2O_2 without a long-lived hydroperoxo intermediate for interception by a substrate. No reaction was observed when **3** and **4** were independently treated with substrates relevant to TS-1 oxidation processes such as diphenylmethanol, phenol, and cyclooctene (See Section 14 in the Supporting Information for experimental details).[7,43] These results are consistent with the lack of catalytic activity observed for **1** and **2** in the presence of H_2O_2.

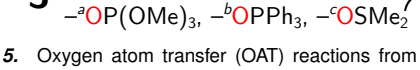

Scheme 5. Oxygen atom transfer (OAT) reactions from $[O_2TiP_4O_{12}]_2^{4-}$ (**3**) to $P(OMe)_3$, PPh_3, and SMe_2 to regenerate the corresponding organic oxide and $[OTiP_4O_{12}]_2^{4-}$ (**1**) under the following conditions: *a*: 23 °C, 10 min, MeCN; *b*: 23 °C, 30 min, MeCN; *c*: 23 °C, 2 h.

We did, however, test the ability of **3** and **4** to behave as stoichiometric oxidants towards phosphorus(III) compounds and sulfides. Treatment of **3** with $P(OMe)_3$, PPh_3 and SMe_2 at ambient temperature resulted in the formation of the corresponding organic oxide as well as clean regeneration of **1** as determined by ^{31}P and ^1H NMR analyses (Scheme 5). Treatment of **4** with PPh_3, however, required heating at 70 °C to generate $OPPh_3$ and **3**. Related vanadium(V) peroxo systems are thermodynmically powerful but kinetically sluggish OAT reagents, and in this respect they are reminiscent of nitrous oxide.[51]

■ CONCLUSIONS

The present metaphosphate complexes represent rare examples of air stable Ti(IV) oxo/peroxo systems containing entirely oxygen based coordination environments at titanium. The metaphosphate ligands support the formation of terminal titanyls as opposed to the

more commonly encountered μ-oxo bridged oligomeric structures, making complexes **1**–**4** molecular models of site isolated titanyl and peroxo units found within heterogeneous oxidation catalysts.

■ EXPERIMENTAL SECTION

General Methods. Unless otherwise stated, all manipulations were performed under open air conditions in the fume hood. $[PPN]_2[P_4O_{12}H_2]$[11] and $[PPN]_2[P_3O_9H]$[12] were prepared as previously reported. All reagents were purchased from Sigma Aldrich (urea·H_2O_2, $[OTi(acac)_2]_2$, 30% H_2O_2), or Gelest ($Me_3SiOOSiMe_3$) and used as received. Acetone (H_2O content < 0.5 w/w%) was purchased from Macron Fine Chemicals, and acetonitrile was purchased from Acros Organics and both were used without further purification. $^{17}OH_2$ (70% enriched) and $^{18}OH_2$ (97% enriched) were purchased from Cambridge Isotope Laboratories, and used as received. IR spectra were recorded on a Bruker Tensor 37 Fourier transform IR (FTIR) spectrometer. Deuterated solvents (D_2O, CD_3CN) were obtained from Cambridge Isotope Laboratories, and used as received. NMR spectra were obtained on a Varian Inova-500 NMR spectrometer with an Oxford Instruments Ltd. superconducting magnet, Bruker Avance 400 instruments equipped with Magnex Scientific superconducting magnets, or on a Varian Mercury 300 spectrometer with an Oxford Instruments Ltd. superconducting magnet. ^1H and $^{13}C\{^1H\}$ NMR spectra are referenced to residual protio-solvent signals. $^{31}P\{^1H\}$ NMR chemical shifts are reported with respect to an external reference (85% H_3PO_4, δ 0.0 ppm), and ^{17}O NMR chemical shifts are externally referenced to D_2O (δ 0.0 ppm). NMR spectra were simulated using the program gNMR version 5.1. ESI-MS(–) data were obtained on a Waters Q-TOF micro mass spectrometer using a source temperature of 100 °C and a desolvation temperature of 150 °C. Mass spectrometry samples were run in neat acetonitrile at concentrations < 1 μM, and the data were processed using the program mMass Version 5.4.1. UV-Vis spectra were collected on an Ocean Optics USB4000 spectrophotometer with a DT-Mini-2GS UV-vis-NIR light source. Elemental analyses were performed by Robertson Microlit Laboratories, Inc (http://www.robertson-microlit.com). X-ray crystallographic details are provided in Section 15.1 of the Supporting Information.

$[PPN]_4[OTiP_4O_{12}]_2$ (**$[PPN]_4$[1]**). To a stirring suspension of $[PPN]_2[P_4O_{12}H_2]$ (350 mg, 0.251 mmol, 1.00 eq) in acetone (7 mL) was added $[OTi(acac)_2]_2$ (72 mg, 0.14 mmol, 0.55 eq) as a solid. MeCN (10 mL) was added dropwise until a homogeneous solution was obtained. The pale yellow reaction mixture was allowed to stir at room temperature (23 °C) for a total of 12 h, at which point the mixture was filtered through a pad of Celite to remove unreacted $[OTi(acac)_2]_2$. The filtrate was concentrated to ca. 3 mL under vacuum, during which time colorless crystals formed on the bottom and sides of the vial. The pale yellow supernatant was removed, and the colorless crystals were washed with acetone (2 mL), and dried under reduced pressure. The supernatant was allowed to stand at room temperature for an additional 24 h to allow a second crop of crystals to grow. These crystals were isolated, washed with acetone (2 mL), and dried under reduced pressure. Total yield: 256 mg, 0.176 mmol, 70%. The solid-state structure determination revealed the presence of one molecule of MeCN and one molecule of acetone per $[PPN]_4[OTiP_4O_{12}]_2$ complex. Elem. Anal. (%) found (calc'd) for $C_{149}H_{129}N_5O_{27}P_{16}Ti_2$ ($[PPN]_4[OTiP_4O_{12}]_2$·MeCN·acetone): C, 59.19 (59.40); H, 4.61 (4.32); N, 2.29 (2.32). ESI-MS(–) (CH_3CN, m/z): 189.88 (calc'd: 189.89). IR (ATR, cm^{-1}) ν: 1262 (s, P=O), 969 (s, Ti≡O). $^{31}P\{^1H\}$ NMR (CD_3CN, 25 °C, 161.9 MHz) δ: 22.20 (s, 8 P, PPN^+), –27.55 (s, 8 P, P_4O_{12}) ppm. ^1H NMR (CD_3CN, 25 °C, 400.1 MHz) δ: 7.48–7.71 (m, 120 H, PPN^+) ppm. $^{13}C\{^1H\}$ NMR (CD_3CN, 25 °C, 100.6 MHz) δ: 134.6 (s, PPN^+), 133.2 (m, PPN^+), 130.4 (m, PPN^+), 128.1 (d, $^1J_{PC}$ = 108 Hz, PPN^+) ppm.

$[PPN]_2[OTiP_3O_9(acac)]$ (**$[PPN]_2$[2]**). To a stirring suspension of $[PPN]_2[P_3O_9H]$ (300 mg, 0.228 mmol, 1.00 eq) in acetone (7 mL) was added $[OTi(acac)_2]_2$ (66 mg, 0.13 mmol, 0.55 eq) as a solid. MeCN (10 mL) was added dropwise until the reaction mixture became homogeneous. The pale yellow reaction mixture was allowed to stir at ambient temperature (23 °C) for a total of 6 h, at which point the pale yellow solution was filtered through a pad of Celite to remove unreacted $[OTi(acac)_2]_2$. All volatiles were then removed under reduced pressure affording a pale yellow residue. The yellow residue was triturated with Et_2O (10 mL), and the Et_2O was subsequently decanted from the resulting solids. The resulting solids were suspended in acetone (5 mL), and filtered away from the pale yellow supernatant. The solids were washed with acetone (3 mL) and dried under reduced pressure, affording $[PPN]_2[OTiP_3O_9(acac)]$ as a cream colored powder (310 mg, 0.210 mmol, 92%). X-ray diffraction quality crystals of $[PPN]_2[OTiP_3O_9(acac)]$ were grown by concentration of the crude reaction mixture by ca. 90% and allowing the resulting mixture to stand at 23 °C. After 12 h, large colorless crystals formed that were isolated and washed with acetone to afford analytically pure $[PPN]_2$[**2**]. Overall yield of crystals: 199 mg, 0.134 mmol, 59%. The solid-state structure determination revealed the presence of one MeCN molecule of crystallization per $[PPN]_2[OTiP_3O_9(acac)]$ complex. Elem. Anal. (%) found (calc'd) for $C_{79}H_{70}N_3O_{12}P_7Ti$ ($[PPN]_2[OTiP_3O_9(acac)]$·MeCN): C, 62.28 (62.61); H, 4.76 (4.65); N, 2.72 (2.77). ESI-MS(–) of $[OTiP_3O_9]^-$ (CH_3CN, m/z): 300.91 (calc'd: 300.82). The complete dianionic complex including the acac ligand is not detectable under ESI-MS(–) conditions, and only the $[OTiP_3O_9]^-$ ion is observed. IR (ATR, cm^{-1}) ν: 1261 (s, P=O), 953 (s, Ti≡O), 933 (s, Ti–O_{acac}). $^{31}P\{^1H\}$ NMR (CD_3CN, 25 °C, 161.9 MHz) δ: 22.20 (s, 4 P, PPN^+), –18.52 (bs, 3 P, P_3O_9) ppm. ^1H NMR (CD_3CN, 25 °C, 400.1 MHz) δ: 7.48–7.71 (m, 60 H, PPN^+), 5.67 (s, 1 H, C*H*), 2.06 (s, 6 H, CH_3) ppm. $^{13}C\{^1H\}$ NMR (CD_3CN, 25 °C, 100.6 MHz) δ: 191.6 (s, *C*=O), 134.6 (s, PPN^+), 133.2 (m, PPN^+), 130.4 (m, PPN^+), 128.1 (d, $^1J_{PC}$ = 108 Hz, PPN^+), 102.6 (s, *C*H), 26.7 (s, *C*H_3) ppm. ^{17}O NMR (MeCN, 25 °C, 68 MHz) δ: 1086 (s, O≡Ti) ppm.

$[PPN]_4[O_2TiP_4O_{12}]_2$ (**$[PPN]_4$[3]**). To a stirring colorless solution of $[PPN]_4$[**1**] (125 mg, 0.0429 mmol, 1.00 eq) in MeCN (5 mL) was added urea hydrogen peroxide (10 mg, 0.11 mmol, 2.4 eq) as a solid. The color of the solution turned orange immediately upon addition. The reaction mixture was allowed to stir at ambient temperature for a total of 10 min, at which point the orange solution was filtered through a pad of Celite to remove the urea byproduct. The orange solution was then concentrated to ca. 0.5 mL. Et_2O (5 mL) was then added until the solution became cloudy. The resulting orange solution was then filtered through a piece of microfiber filter paper and the filtrate was allowed to stand at 23 °C for 12 h, during which time large diffraction quality orange crystals grew. The pale orange supernatant was removed and the crystals were dried under reduced pressure to afford analytically pure $[PPN]_4[O_2TiP_4O_{12}]_2$. Yield: 77 mg, 0.026 mmol, 61%. The solid-state structure determination revealed six MeCN molecules of crystallization per $[PPN]_4[O_2TiP_4O_{12}]_2$ complex. Elem. Anal. (%) found (calc'd) for $C_{156}H_{138}N_{10}O_{28}P_{16}Ti_2$ ($[PPN]_4[O_2TiP_4O_{12}]_2$·6MeCN): C, 57.98 (58.70); H, 4.41 (4.36); N, 3.76 (4.39). The most likely explanation for the discrepancies in the C and N analyses are due to variable acetonitrile content within the voids of the crystal lattice (Section 15.1 in the Supporting Information). ESI-MS(–) of $[O_2TiP_4O_{12}]^{2-}$

(CH_3CN, m/z): 197.95 (calc'd: 197.89). IR (ATR, cm^{-1}) ν: 1262 (s, P=O), 884 (s, O–O). $^{31}P\{^1H\}$ NMR (CD_3CN, 25 °C, 161.9 MHz) δ: 22.20 (s, 8 P, PPN^+), –28.09 (s, 8 P, P_4O_{12}) ppm. ^1H NMR (CD_3CN, 25 °C, 400.1 MHz) δ: 7.48–7.71 (m, 120 H, PPN^+) ppm. $^{13}C\{^1H\}$ NMR (CD_3CN, 25 °C, 100.6 MHz) δ: 134.6 (s, PPN^+), 133.2 (m, PPN^+), 130.4 (m, PPN^+), 128.1 (d, $^1J_{PC}$ = 108 Hz, PPN^+) ppm. UV-Vis; λ_{max} (ε): 379 nm (1104 $M^{-1}cm^{-1}$).

Alternative preparation using $(SiMe_3)_2O_2$. In the fumehood, to a stirring solution of $[PPN]_4$[**1**] (100 mg, 0.0340 mmol, 1.00 eq) in MeCN (5 mL) was added $(SiMe_3)_2O_2$ (18 μL, 0.086 mmol, 2.5 eq) via 50 μL microsyringe. The color of the solution gradually changed from colorless to bright orange over the course of 12 h, at which point the reaction mixture was concentrated to ca. 1 mL. To the concentrated solution was added Et_2O (15 mL) in order to precipitate orange solids. The solids were isolated by filtration, washed with Et_2O (15 mL), and dried under reduced pressure affording $[PPN]_4$[**3**] as an orange solid. Yield: 85 mg, 0.029 mmol, 86%.

$[PPN]_2[O_2TiP_3O_9(acac)]$ ($[PPN]_2$[**4**]). To a stirring colorless solution of $[PPN]_2$[**2**] (100 mg, 0.0677 mmol, 1.00 eq) was added a solution of 30% H_2O_2 (10 μL, 0.098 mmol, 1.4 eq) via 10 μL syringe. The color of the solution immediately changed from colorless to bright orange upon complete addition. The orange solution was allowed to stir at ambient temperature for a total of 10 min, at which point all volatiles were removed under reduced pressure. The resulting orange residue was triturated with THF (5 mL), and then the THF was subsequently decanted away from the orange solids. The solids were then dissolved in MeCN (1 mL), and then Et_2O (3 mL) was added until the solution became cloudy. The orange solution was then filtered through a piece of microfiber filter paper and allowed to stand at ambient temperature (23 °C). Large diffraction quality orange crystals grew over the course of 12 h. The pale orange mother liquor was removed and the crystals were dried under reduced pressure to afford analytically pure $[PPN]_2[O_2TiP_3O_9(acac)]$. Yield: 66 mg, 0.044 mmol, 65%. The solid-state structure shows one Et_2O molecule of crystallization per $[PPN]_2[O_2TiP_3O_9(acac)]$ complex. Elem. Anal. (%) found (calc'd) for $C_{81}H_{77}N_2O_{14}P_7Ti$ ($[PPN]_2[O_2TiP_3O_9(acac)]\cdot Et_2O$): C, 61.69 (61.95); H, 4.37 (4.52); N, 2.07 (1.88). ESI-MS(–) of $[O_2TiP_3O_9]^-$ (CH_3CN, m/z): 316.82 (calc'd: 316.81). The complete dianionic complex including the acac ligand is not detectable under ESI-MS(–) conditions, and only the $[O_2TiP_3O_9]^-$ ion is observed. IR (ATR, cm^{-1}) ν: 1251 (s, P=O), 934 (s, Ti–O_{acac}), 903 (O–O). $^{31}P\{^1H\}$ NMR (CD_3CN, 25 °C, 161.9 MHz) δ: 22.20 (s, 4 P, PPN^+), –17.73 (s, 3 P, P_3O_9) ppm. ^1H NMR (CD_3CN, 25 °C, 400.1 MHz) δ: 7.48–7.71 (m, 60 H, PPN^+), 5.52 (s, 1 H, C*H*) ppm. The CH_3 resonance overlaps with CD_3CN solvent. $^{13}C\{^1H\}$ NMR (CD_3CN, 25 °C, 100.6 MHz) δ: 190.2 (s, *C*=O) 134.6 (s, PPN^+), 133.2 (m, PPN^+), 130.4 (m, PPN^+), 128.1 (d, $^1J_{PC}$ = 108 Hz, PPN^+), 102.3 (s, *C*H), 26.6 (s, *C*H_3) ppm. UV-Vis; λ_{max} (ε): 403 nm (674 $M^{-1}cm^{-1}$).

Alternative preparation using $(SiMe_3)_2O_2$. In the fumehood, to a stirring solution of $[PPN]_2$[**3**] (100 mg, 0.0677 mmol, 1.00 eq) in MeCN (5 mL) was added $(SiMe_3)_2O_2$ (22 μL, 0.10 mmol, 1.5 eq) via 50 μL microsyringe. The color of the solution gradually changed from colorless to bright orange over the course of 12 h, at which point the reaction mixture was concentrated to ca. 1 mL. To the concentrated solution was added Et_2O (15 mL) in order to precipitate orange solids. The solids were isolated by filtration, washed with Et_2O (15 mL), and dried under reduced pressure affording $[PPN]_2$[**4**] as an orange solid. Yield: 90 mg, 0.060 mmol, 90%.

Acknowledgement This work was supported by NSF under the NSF Center CHE-1305124. Yanfeng Jiang is thanked for assistance with X-ray crystallography, and Wesley Transue and Shiyu Zhang are thanked for assistance with VT-NMR experiments.

Supporting Information Available: Experimental details and characterization data for all compounds including crystallographic information for $[PPN]_4$[**1**], $[PPN]_2$[**2**], $[PPN]_4$[**3**], and $[PPN]_2$[**4**] are provided in the Supporting Information. This material is available free of charge via the Internet at http://pubs.acs.org.

References

(1) (a) Collins, T. J. TAML Oxidant Activators: A New Approach to the Activation of Hydrogen Peroxide for Environmentally Significant Problems. *Acc. Chem. Res.* **2002**, *35*, 782–790; (b) Nam, W. High-Valent Iron(IV)-Oxo Complexes of Heme and Non-Heme Ligands in Oxygenation Reactions. *Acc. Chem. Res.* **2007**, *40*, 522–531.

(2) (a) Sheldon, R. A.; Wallau, M.; Arends, I. W. C. E.; Schuchardt, U. Heterogeneous Catalysts for Liquid-Phase Oxidations: Philosophers' Stones or Trojan Horses? *Acc. Chem. Res.* **1998**, *31*, 485–493; (b) Arends, I.; Sheldon, R. Activities and Stabilities of Heterogeneous Catalysts in Selective Liquid Phase Oxidations: Recent Developments. *Appl. Catal., A* **2001**, *212*, 175–187.

(3) Wilson, S. L.; Jones, C. W. Solid Solutions for Cleaning up Chemical Processes Using Hydrogen Peroxide. In *Proceedings of the 3rd World Congress on Oxidation Catalysis*; R.K. Grasselli, A. G., S.T. Oyama, Lyons, J., Eds.; Elsevier, 1997; Vol. Volume 110, pp 603–613.

(4) (a) Sheldon, R. A. In *Organic Peroxygen Chemistry*; Herrmann, W. A., Ed.; Springer Berlin Heidelberg, 1993; pp 21–43; (b) Notari, B. Titanium Silicalites. *Catal. Today* **1993**, *18*, 163–172.

(5) (a) Taramasso, M.; Perego, G.; Notari, B., 1983, US Patent 4,410,501; (b) Clerici, M. G. In *Titanium Silicalite-1*; Wiley-VCH Verlag GmbH & Co. KGaA, 2009; pp 705–754.

(6) Clerici, M. The Activity of Titanium Silicalite-1 (TS-1): Some Considerations on its Origin. *Kinet. Catal.* **2015**, *56*, 450–455.

(7) (a) Bordiga, S.; Bonino, F.; Damin, A.; Lamberti, C. Reactivity of Ti(IV) Species Hosted in TS-1 Towards H_2O_2-H_2O Solutions Investigated by Ab Initio Cluster and Periodic Approaches Combined with Experimental XANES and EXAFS Data: A Review and New Highlights. *Phys. Chem. Chem. Phys.* **2007**, *9*, 4854–4878; (b) Corma, A. State of the Art and Future Challenges of Zeolites as Catalysts. *J. Catal.* **2003**, *216*, 298–312.

(8) Wang, K.-Y.; Lin, Z.; Bassil, B. S.; Xing, X.; Haider, A.; Keita, B.; Zhang, G.; Silvestru, C.; Kortz, U. Ti_2-Containing 18-Tungsto-2-Arsenate(III) Monolacunary Host and the Incorporation of a Phenylantimony(III) Guest. *Inorg. Chem.* **2015**, *54*, 10530–10532.

(9) Kholdeeva, O. A.; Donoeva, B. G.; Trubitsina, T. A.; Al-Kadamany, G.; Kortz, U. Unique Catalytic Performance of the Polyoxometalate $[Ti_2(OH)_2As_2W_{19}O_{67}(H_2O)]^{8-}$: The Role of 5-Coordinated Titanium in H_2O_2 Activation. *Eur. J. Inorg. Chem.* **2009**, *2009*, 5134–5141.

(10) Antonova, N. S.; Carbó, J. J.; Kortz, U.; Kholdeeva, O. A.; Poblet, J. M. Mechanistic Insights into Alkene Epoxidation with H_2O_2 by Ti- and Other TM-Containing Polyoxometalates: Role of the Metal Nature and Coordination Environment. *J. Am. Chem. Soc.* **2010**, *132*, 7488–7497.

(11) Jiang, Y.; Chakarawet, K.; Kohout, A. L.; Nava, M.; Marino, N.; Cummins, C. C. Dihydrogen Tetrametaphosphate, $[P_4O_{12}H_2]^{2-}$: Synthesis, Solubilization in Organic Media, Preparation of its Anhydride $[P_4O_{11}]^{2-}$ and Acidic Methyl Ester, and Conversion to Tetrametaphosphate Metal Complexes via Protonolysis. *J. Am. Chem. Soc.* **2014**, *136*, 11894–11897.

(12) Chakarawet, K.; Knopf, I.; Nava, M.; Jiang, Y.; Stauber, J. M.; Cummins, C. C. Crystalline Metaphosphate Acid Salts: Synthesis in Organic Media, Structures, Hydrogen-Bonding Capability, and Implication of Superacidity. *Inorg. Chem.* **2016**, *55*, 6178–6185.

(13) (a) Yamamoto, A.; Kambara, S. Structures of the Reaction Products of Tetraalkoxytitanium with Acetylacetone and Ethyl Acetoacetate. *J. Am. Chem. Soc.* **1957**, *79*, 4344–4348; (b) Smith, G. D.; Caughlan, C. N.; Campbell, J. A. Crystal and molecular structures of di-μ-Oxo-bis(diacetylacetonatotitanium(IV))-bisdioxane, $(TiO(C_5H_7O_2)_2)_2\cdot 2C_4H_8O_2$, di-$\mu$-Oxo-bis(diacetylacetonatotitanium(IV)), $(TiO(C_5H_7O_2)_2)_2$. *Inorg. Chem.* **1972**, *11*, 2989–2993.

(14) (a) Graetzel, M.; Rotzinger, F. P. Raman Spectroscopic Evidence for the Existence of Titanyl (TiO^{2+}) in Acidic Aqueous Solutions. *Inorg. Chem.* **1985**, *24*, 2320–2321; (b) Hill, J. E.; Fanwick, P. E.; Rothwell, I. P. Isolation and Characterization of Bis(2,6-diisopropylphenoxo)bis(4-pyrrolidinopyridine)oxotitanium: A Mononuclear Aryloxide Compound Containing a Terminal Titanium(IV)-oxo Group. *Inorg. Chem.* **1989**, *28*, 3602–3604.

(15) Housmekerides, C. E.; Ramage, D. L.; Kretz, C. M.; Shontz, J. T.; Pilato, R. S.; Geoffroy, G. L.; Rheingold, A. L.; Haggerty, B. S. Addition and Cycloaddition Reactions of the Nucleophilic Oxo and Sulfido Complexes [tmtaa]Ti=X (X = O, S; tmtaa = Dianion of 7,16-dihydro-6,8,15,17-tetramethyldibenzo[b,i][1,4,8,11]tetraazacyclotetradecine). *Inorg. Chem.* **1992**, *31*, 4453–4468.

(16) Dwyer, P. N.; Puppe, L.; Buchler, J. W.; Scheidt, W. R. Molecular Stereochemistry of (α,γ-dimethyl-α,γ-dihydrooctaethylporphinato)oxotitanium(IV). *Inorg. Chem.* **1975**, *14*, 1782–1785.

(17) Bodner, A.; Jeske, P.; Weyhermueller, T.; Wieghardt, K.; Dubler, E.; Schmalle, H.; Nuber, B. Mono- and Dinuclear Titanium(III)/Titanium(IV)

Complexes with 1,4,7-trimethyl-1,4,7-triazacyclononane (L). Crystal Structures of a Compositionally Disordered Green and a Blue Form of $[LTiCl_3]$. Structures of $[LTi(O)(NCS)_2]$, $[LTi(OCH_3)Br_2](ClO_4)$, and $[L_2Ti_2(O)_2F_2(\mu\text{-}F)](PF_6)$. *Inorg. Chem.* **1992**, *31*, 3737–3748.
(18) F. Albert Cotton, C. A. M. M. B., Geoffrey Wilkinson In *Advanced Inorganic Chemistry*; Wiley-Interscience, 1988; p 656.
(19) Kamimura, S.; Matsunaga, T.; Kuwata, S.; Iwasaki, M.; Ishii, Y. Synthesis, Structures, and Solution Behavior of Di- and Trinuclear Titanium(IV)−Cyclophosphato Complexes. *Inorg. Chem.* **2004**, *43*, 6127–6129.
(20) Mendiratta, A.; Figueroa, J. S.; Cummins, C. C. Synthesis of a Four-coordinate Titanium(IV) Oxoanion via Deprotonation and Decarbonylation of Complexed Formate. *Chem. Commun.* **2005**, 3403–3405.
(21) Liu, Q.-X.; Zhou, Z.-H. Monomeric Peroxo Titanate Coordinated with Cyclohexanediaminetetraacetate: Towards the Active Oxygen Species of the Ti(IV) Site Hosted in the Titanium Silicalite Catalyst TS-1. *Polyhedron* **2012**, *35*, 1–6.
(22) Mayer, J. M. Metal-Oxygen Multiple Bond Lengths: A Statistical Study. *Inorg. Chem.* **1988**, *27*, 3899–3903.
(23) Pyykkö, P.; Atsumi, M. Molecular Double-Bond Covalent Radii for Elements Li-E112. *Chem. Eur. J.* **2009**, *15*, 12770–12779.
(24) (a) Ballhausen, C. J.; Gray, H. B. The Electronic Structure of the Vanadyl Ion. *Inorg. Chem.* **1962**, *1*, 111–122; (b) Winkler, J. R.; Gray, H. B. In *Electronic Structures of Oxo-Metal Ions*; Springer Berlin Heidelberg, 2012; pp 17–28.
(25) Spek, A. L. Structure Validation in Chemical Crystallography. *Acta Cryst.* **2009**, *D65*, 148–155.
(26) Garner, C. D. The Early Transition Metals. In *Inorganic Chemistry of the Transition Elements: Volume 1*; Johnson, B. F. G., Ed.; The Royal Society of Chemistry, 1972; Vol. 1, pp 1–122.
(27) Wong, E. H.; Sun, X.; Gabe, E. J.; Lee, F. L.; Charland, J. P. Coordination Complexes Derived from Tri-, Tetra-, and Pentaphosphoxane Rings. *Organometallics* **1991**, *10*, 3010–3020.
(28) Fujii, H.; Kurahashi, T.; Tosha, T.; Yoshimura, T.; Kitagawa, T. ^{17}O NMR Study of Oxo Metalloporphyrin Complexes: Correlation with Electronic Structure of MO Moiety. *J. Inorg. Biochem.* **2006**, *100*, 533–541.
(29) Comba, P.; Merbach, A. The Titanyl Question Revisited. *Inorg. Chem.* **1987**, *26*, 1315–1323.
(30) (a) Talsi, E.; Shalyaev, K. ^1H and ^{17}O NMR Spectroscopic Detection and Characterization of Titanium(IV) Alkylperoxo Complex. *J. Mol. Catal. A: Chem.* **1996**, *105*, 131–136; (b) Blanchard, J.; Ribot, F.; Sanchez, C.; Bellot, P.-V.; Trokiner, A. Structural Characterization of Titanium-oxo-polymers Synthesized in the Presence of Protons or Complexing Ligands as Inhibitors. *J. Non-Cryst. Solids* **2000**, *265*, 83–97.
(31) Goedken, V. L.; Ladd, J. A. New Macrocyclic Complexes of Titanium(IV): Synthesis, Reactivity, and X-ray Crystal Structure of the Trigonal Prismatic $Ti(C_{22}H_{22}N_4)Cl_2$, and Synthesis and Reactivity of its Peroxo, Disulphido, and Pyrocatecholato Derivatives. *J. Chem. Soc., Chem. Commun.* **1982**, 142–144.
(32) Kisko, J. L.; Hascall, T.; Parkin, G. Multiple Bonding of Titanium and Vanadium to the Heavier Chalcogens: Syntheses and Structures of the Terminal Selenido and Tellurido Complexes $[\eta^4\text{-}Me_8taa]ME$ (M = Ti, V; E = Se, Te). *J. Am. Chem. Soc.* **1997**, *119*, 7609–7610.
(33) (a) Dong, S.; Bao, C.; Tian, H.; Yan, D.; Geng, Y.; Wang, F. ABAB-Symmetric Tetraalkyl Titanyl Phthalocyanines for Solution Processed Organic Field-Effect Transistors with Mobility Approaching 1 $cm^2\ V^{-1}\ s^{-1}$. *Adv. Mater.* **2013**, *25*, 1165–1169; (b) Seikel, E.; Grau, M.; Käsmarker, R.; Oelkers, B.; Sundermeyer, J. Synthesis and Crystal Structure of Novel, Soluble Titanyl Phthalocyanines. *Inorg. Chim. Acta* **2011**, *374*, 119–126; (c) Konarev, D. V.; Kuzmin, A. V.; Faraonov, M. A.; Ishikawa, M.; Khasanov, S. S.; Nakano, Y.; Otsuka, A.; Yamochi, H.; Saito, G.; Lyubovskaya, R. N. Synthesis, Structures, and Properties of Crystalline Salts with Radical Anions of Metal-Containing and Metal-Free Phthalocyanines. *Chem. Eur. J.* **2015**, *21*, 1014–1028.
(34) Jeske, P.; Haselhorst, G.; Weyhermueller, T.; Wieghardt, K.; Nuber, B. Synthesis and Characterization of Mononuclear Octahedral Titanium(IV) Complexes Containing Ti=O, $Ti(O_2)$, and $Ti(OCH_3)_x$ (x = 1-3) Structural Units. *Inorg. Chem.* **1994**, *33*, 2462–2471.
(35) R. Galsworthy, J.; L. H. Green, M.; Muller, M.; Prout, K. Reactions of Transition-metal Oxo Complexes with $B(C_6F_5)_3$: Crystal Structures of $[VO(B(C_6F_5)_3)(acac)_2]$, $[TiO(B(C_6F_5)_3)(acac)_2]$ and $cis\text{-}[MoO(O(B(C_6F_5)_3))(acac)_2]$ (acac = acetylacetonate). *J. Chem. Soc., Dalton Trans.* **1997**, 1309–1314.
(36) Rabe, S.; Müller, U. Oxotitan-Addukte mit Dimethylsulfoxid: $[TiO(OSMe_2)_5]Cl_2$ und $[Ti_4O_6(OSMe_2)_{12}]Cl_4{\cdot}5Me_2SO{\cdot}1/2\ H_2O$ / Oxotitanium Compounds with Dimethylsulfoxide: $[TiO(OSMe_2)_5]Cl_2$ and $[Ti_4O_6(OSMe_2)_{12}]Cl_4{\cdot}5Me_2SO{\cdot}1/2\ H_2O$. *Z. Naturforsch., B: Chem. Sci.* **1997**, *52*, 1291–1295.
(37) Li, P.-J.; Huang, S.-H.; Huang, K.-Y.; Ru-Ji, W.; Mak, T. C. Crystal Structure of Tetraguanidinium Tri(carbonato)oxotitanium(IV) Dihydrate, $[C(NH_2)_3]_4[TiO(CO_3)_3]{\cdot}2H_2O$. *Inorg. Chim. Acta* **1990**, *175*, 105–110.
(38) Schwarzenbach, G.; Muehlebach, J.; Mueller, K. Peroxo Complexes of Titanium. *Inorg. Chem.* **1970**, *9*, 2381–2390.
(39) (a) Mimoun, H.; Postel, M.; Casabianca, F.; Fischer, J.; Mitschler, A. Novel Unusually Stable Peroxotitanium(IV) Compounds. Molecular and Crystal Structure of Peroxobis(picolinato)(hexamethylphosphoric triamide)titanium(IV). *Inorg. Chem.* **1982**, *21*, 1303–1306; (b) Wang, G.-C.; Sung, H. H. Y.; Williams, I. D.; Leung, W.-H. Tetravalent Titanium, Zirconium, and Cerium Oxo and Peroxo Complexes Containing an Imidodiphosphinate Ligand. *Inorg. Chem.* **2012**, *51*, 3640–3647.
(40) Guilard, R.; Latour, J. M.; Lecomte, C.; Marchon, J. C.; Protas, J.; Ripoll, D. Peroxotitanium(IV) Porphyrins. Synthesis, Stereochemistry, and Properties. *Inorg. Chem.* **1978**, *17*, 1228–1237.
(41) Clerici, M. G. Oxidation of Saturated Hydrocarbons with Hydrogen Peroxide, Catalysed by Titanium Silicalite. *Appl. Catal.* **1991**, *68*, 249–261.
(42) Hulea, V.; Moreau, P.; Di Renzo, F. Thioether Oxidation by Hydrogen Peroxide Using Titanium-containing Zeolites as Catalysts. *J. Mol. Catal. A: Chem.* **1996**, *111*, 325–332.
(43) Clerici, M.; Bellussi, G.; Romano, U. Synthesis of Propylene Oxide from Propylene and Hydrogen Peroxide Catalyzed by Titanium Silicalite. *J. Catal.* **1991**, *129*, 159–167.
(44) Xu, M.; Bunes, B. R.; Zang, L. Paper-Based Vapor Detection of Hydrogen Peroxide: Colorimetric Sensing with Tunable Interface. *ACS Appl. Mater. Interfaces* **2011**, *3*, 642–647.
(45) Dakanali, M.; Kefalas, E. T.; Raptopoulou, C. P.; Terzis, A.; Voyiatzis, G.; Kyrikou, I.; Mavromoustakos, T.; Salifoglou, A. A New Dinuclear Ti(IV)-Peroxo-Citrate Complex from Aqueous Solutions. Synthetic, Structural, and Spectroscopic Studies in Relevance to Aqueous Titanium-Peroxo-Citrate Speciation. *Inorg. Chem.* **2003**, *42*, 4632–4639.
(46) Kholdeeva, O. A.; Trubitsina, T. A.; Maksimovskaya, R. I.; Golovin, A. V.; Neiwert, W. A.; Kolesov, B. A.; López, X.; Poblet, J. M. First Isolated Active Titanium Peroxo Complex: Characterization and Theoretical Study. *Inorg. Chem.* **2004**, *43*, 2284–2292.
(47) (a) Wang, G.-C.; Sung, H. H. Y.; Williams, I. D.; Leung, W.-H. Tetravalent Titanium, Zirconium, and Cerium Oxo and Peroxo Complexes Containing an Imidodiphosphinate Ligand. *Inorg. Chem.* **2012**, *51*, 3640–3647; (b) Rohe, M.; Merz, K. Active Peroxo Titanium Complexes: Syntheses, Characterization and their Potential in the Photooxidation of 2-Propanol. *Chem. Commun.* **2008**, 862–864.
(48) Notari, B. Microporous Crystalline Titanium Silicates. In *Microporous Crystalline Titanium Silicates*; D.D. Eley, W. O. H., Gates, B., Eds.; Academic Press, 1996; Vol. Volume 41, pp 253–334.
(49) Busch, D. H.; Yin, G.; Lee, H.-J. In *Mechanisms in Homogeneous and Heterogeneous Epoxidation Catalysis*; Oyama, S. T., Ed.; Elsevier: Amsterdam, 2008; pp 119–153.
(50) Boro, B. J.; Lansing, R.; Goldberg, K. I.; Kemp, R. A. Reaction of a Monomeric Titanium Hydride with Dioxygen does not Produce a Stable Titanium Hydroperoxide. *Inorg. Chem. Commun.* **2011**, *14*, 531–533.
(51) Cozzolino, A. F.; Tofan, D.; Cummins, C. C.; Temprado, M.; Palluccio, T. D.; Rybak-Akimova, E. V.; Majumdar, S.; Cai, X.; Captain, B.; Hoff, C. D. Two-Step Binding of O_2 to a Vanadium(III) Trisanilide Complex To Form a Non-Vanadyl Vanadium(V) Peroxo Complex. *J. Am. Chem. Soc.* **2012**, *134*, 18249–18252.

Table of Contents Entry

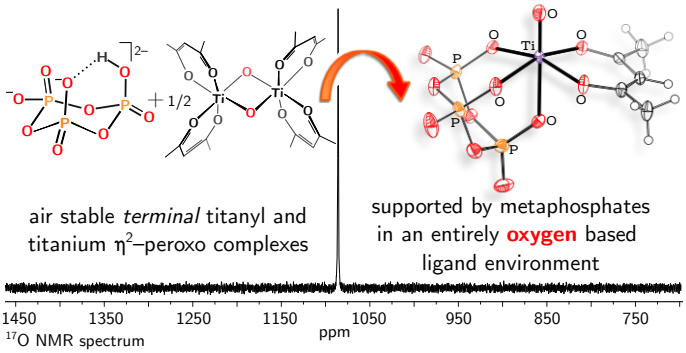

A new pair of air stable terminal titanyl complexes supported by tri- and tetrametaphosphate ligands is reported. These compounds react with H_2O_2 to generate the corresponding peroxo complexes with loss of water, and represent rare examples of terminal titanium(IV) oxos stabilized by an all-oxygen ligand field.